e-Polymers **2006**, no. 054

http://www.e-polymers.org
ISSN 1618-7229

Synthesis and some Mechanical Properties of Polysulfobetaine – Polyacrylamide Double Networks

George Georgiev,[1] Konstantina Dyankova,[1] Elena Vassileva,[1] Klaus Friedrich[2]*

[1]Faculty of Chemistry, University of Sofia, 1 J. Bourchier Ave., 1164 Sofia, Bulgaria; e-mail: georgs@chem.uni-sofia.bg
[2]Institute for Composite Materials, University of Kaiserslautern, 58 Erwin-Schrödinger Ave., 67663 Kaiserslautern, Germany; e-mail: klaus.friedrich@ivw.uni-kl.de

(Received: 4 February, 2006; published: 20 August, 2006)

Abstract: Double polymer networks (DNs) with poly(N-(3-sulfopropyl)-N-methacroyloxyethyl-N,N-dimethylammonium betaine) component as a high density cross-linking agent were synthesized by thermoinitiated cross-linking polymerization. Good mechanical properties of the produced DNs were established. These, in combination with an excellent biocompatibility of polyzwitterions, open a possibility for wide biomedical applications of these materials. It is also shown that the mechanical properties could be controlled by the factors (cross-linking agent and monomer concentrations, temperature and time for the cross-linking polymerization, order of single network formation) influencing the junction point densities of the two single networks and on the microphase separation taking place during the formation of the second single network. Specific dipole-dipole interaction between polyzwitterion monomer units as a reason for this separation is a distinct peculiarity of poly(N-(3-sulfopropyl)-N-methacroyloxyethyl-N,N-dimethylammoniumbetaine)/poly(acrylamide) double networks in comparison to poly(2-acrylamido-2-methylpropanesulfonic-acid)/poly(acrylamide) ones.

Introduction

Double polymer networks (DN) are special types of interpenetrating networks (IPN), which consist of single networks (SN) strongly differing in their cross-linking density and in the length and the stiffness of their intercross-linking segments (Mott et al. [1], Gong et al., [2]). The network with a high degree of cross-linking (HDSN) plays the role of a composite filler, imparting hardness and strength to the DN, while the low density network (LDSN) represents an isotropic polymer matrix. Their advantage is the possibility to change (within a wide range) their physical and mechanical properties as a function of specific guiding parameters, such as the monomer ratio, the initiator and cross-linking agent nature and concentration, the cross-linking time and temperature, the order of performance of the two polymerizations, the nature and thermodynamic compatibility of the two SN and the degree of swelling of the first SN in the solution of the monomer of the second one (Gong et al. [2]). Recently, it was established that the hydrogels of DN of poly(2-acrylamido-2-methylpropanesulfonic-acid) (PAMPS) and poly(acrylamide) (PAAm) have very high elastic and shear modulus values at definite concentration ratios of the two monomers and the monomers and the cross-linking agents (Gong et al. [2]). These results open opportunities for biomedical applications of DN, combining their good mechanical properties with the necessary to this end, DN biocompatibility. During the last decade**,** polyzwitterions (PZ) (polysulfo- and polyphosphobetaines) are imposed as synthetic polymers with excellent biocompatibility, finding applications as non-trombogenic prostheses, membranes, catheters, joint degeneration retardants, enzyme stabilizers, qualitative cosmetic compositions (Lowe et al. [3], Ishihara et al. [4]). Hence, it is interesting to synthesize and characterize DN with PZ as a single network (SN). In the work presented here, the first results on the synthesis of DN with PZ as one of the two SNs; their microhardness, elastic modulus and morphological homogeneity as dependent on the HDSN and LDSN junction point densities are reported. From the theoretical point of view, the change of the PAMPS SN by PDMAPS is of crucial interest, since the repulsive PAMPS monomer units are changed by the attractive (via dipole-dipole interaction) PDMAPS ones. It is interesting to establish the extent to which this change will influence the optimal conditions for DN synthesis, and the drastic improvement of the DNs mechanical properties as comparison to those of the SNs.

Results and discussion

DN dry sample characterization

The results from the microhardness measurements, together with the equilibrium swelling ratios, are presented in Table 1. The following conclusions about the influences of the different parameters of DN synthesis on these properties could be drawn from the above mentioned results:

(1) As expected increasing the cross-linking agent concentration used for HDSN formation results in an increasing microhardness of the DN. This increase is most probably due to the increased total cross-linking density of the DNs, suggested by both the higher cross-linking agent concentration for HDSN and the increased mutual interpenetration of the two single networks. This is confirmed by the equilibrium swelling ratios of the samples (Table 1). The network densities of DNs obviously increase and the equilibrium swelling ratios decrease with the rise of the cross-linking agent concentration. Compared to the HDSN (PDMAPS), the equilibrium swelling of the two DNs is greater. This is in full agreement with the 20-fold difference between the swelling abilities of the two single networks, in favour of PAAm SN (LDSN). The insertion of the higher-swelling LDSN to the considerably lower-swelling HDSN (PDMAPS) as a component of the DNs results in a considerable increase of the DN equilibrium swelling, as compared to that of the initial HDSN.

The high microhardness value of LDSN is quite surprising. It could be explained by the elasticity of this network, which is the more elastic component in the total deformation of the material under loading. As a result, the elastic recovery after unloading is higher and the measured imprint diagonals are smaller than the real ones. In contrast, HDSN had the lowest microhardness value, as compared to all other samples, but this value is not realistic since the dried HDSN samples were very brittle and broke during the microhardness testing procedure.

(2) The second parameter of DN synthesis that has been varied was the cross-linking density for LDSN, which was changed by varying the monomer/cross-linking agent ratio used for LDSN formation. As it is seen in Table 1, line **II**, with the rise of this ratio the DN microhardness decreases, even though this decrease is almost within the experimental error. This is explained by the looser network of the LDSN, as

confirmed by the higher equilibrium swelling ratio for the DN PDMAPS 1.0;5.0/PAAm ***3.0***;0.1 (242%), as compared to the DN PDMAPS 1.0;5.0/PAAm ***2.0***;0.1 (196%).

Tab. 1. Vicker’s microhardness measured for dry samples along with the equilibrium swelling ratios.

Sample	Microhardness in MPa	Equilibrium swelling ratio in %
I. Influence of the cross-linking agent concentration used to form HDSN		
PDMAPS 1.0;***5.0***/PAAm 2.0;0.1	175±27	196
PDMAPS 1.0;***3.0***/PAAm 2.0;0.1	74±5	300
II. Influence of the monomer concentration ratio in the two SNs and of LDSN cross-linking density		
PDMAPS 1.0;5.0/PAAm ***2.0***;0.1	175±27	196
PDMAPS 1.0;5.0/PAAm ***3.0***;0.1	162±11	242
III. Influence of the reverse order of DM formation		
PDMAPS 1.0;4.0/PAAm 2.0;0.1 **(“straight” DN)**	84±4	279
PAAm 2.0;0.1/PDMAPS 1.0;4.0 **(“reverse” DN)**	117±13 (**38**)****	391
IV. Influence of the time for HDSN cross-linking		
PDMAPS 1.0;4.0-***1h***/PAAm 2.0;0.1***	76±5	504
PDMAPS 1.0;4.0–***5.5h***/PAAm 2.0;0.1***	84±4	279
V. SN characteristics		
PAAm 2.0;0.1 (LDSN)	307±13 (**16**)****	2124
PDMAPS 1.0;4.0 (HDSN)	33.3±0.7**	116

* The varied parameters for the different DNs are marked with **bold** and *italic.*

** This value is not realistic, since the dried HDSN was very brittle and broke during the microhardness testing.

*** Time of cross-linking for the HDSN.

**** The values in brackets are obtained by the correction of the measured ones, accounting for the elastic recovery.

(3) The order of SN formation has a strong effect on the microhardness of the DN (Table 1, line III). The **“straight”** and the **“reverse”** DN have approximately the same composition and differ only in the order of SN formation. However, the **“reverse”** DN has a lower real microhardness and higher swelling ratio than the **“straight”** one. This difference could be attributed to the different structural organization of the two DNs.

As one can see in Fig. 1, if PAAm SN is second in the order of formation, the structure is more uniform (Fig. 1A) than that produced if the HDSN (PDMAPS) is second in the order of formation (Fig. 1B). The size of the PAAM white isles (e.g., Sawyer et al. [8]) in the “straight” DN (Fig. 1A) are below 100 nm, while that of the same isles formed as a result of microphase separation in the “reverse” DN are around 200-300 nm. These large PAAm isles ensure a higher swelling ratio value and lower microhardness of the “reverse” DN.

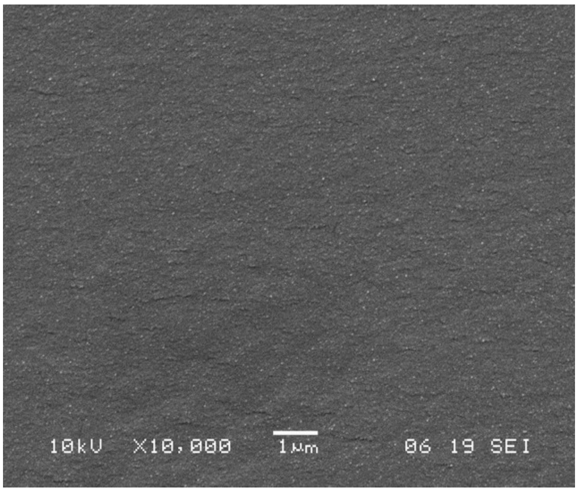

A

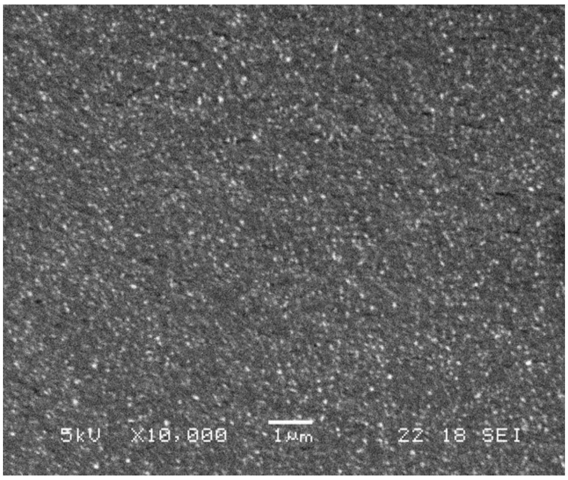

B

Fig. 1. SEM micrographs of “straight” DN PDMAPS 1.0;4.0/PAAm 2.0;0.1 **(A)** and “reverse” DN PAAm 2.0;0.1/PDMAPS 1.0;4.0 **(B).** Magnification 10 000 X.

The reason for the different PAAM isle sizes and size distributions in the “straight” and “reverse” DNs is most probably the self-organization ability of the zwitterionic monomer units to form clusters with the opposite- oriented dipoles [9]. During the formation of the “straight” network, such clusters provide an additional physical cross-linking of the first HDSN, which hampers the penetration of the second monomer (AAm) in the HDSN. This penetration proceeds for a longer time and the formation of the regions (isles) of cross-linked PAAm is less probable. The situation is quite different during the formation of the “inverse” DN, where the first forming network is the PAAm LDSN. In this case, such additional physical cross-linking is impossible and the pores for the diffusion of the second monomer (PDMAPS) are large. Upon saturation of this loose network, the PDMAPS molecules could be uniformly distributed. However, the physical crosslinking between the PDMAPS monomer units proceeds before or together with the second chemical cross-linking reaction. The clusters of the PDMAPS monomer units form separate microdomains, and in this way the PAAm SN is less destroyed; larger PAAm isles are formed than in the case of the "straight" DNs. To check this microseparation mechanism, a comparison of the characteristics of the two DNs with the same composition is necessary. This is achieved by the use of gravimetrically analyzed (under vacuum at room temperature) DNs after each cross-linking polymerization. The networks with the closest compositions are used.

(4) In order to ensure a better mutual penetration of both SNs, we have varied the time of cross-linking used for the HDSN formation (Table 2, line IV) **1 h** and **5.5 h**, respectively, were chosen as cross-linking times for the HDSN. The shorter time resulted in a viscous fluid containing a very thin gelated HDSN layer, while the longer time ensured a well defined gel structure in the HDSN. Then the components of the LDSN have been added, and it was formed as usual for **8 h** of cross-linking. Rigid DN gels were obtained in both cases. The difference between these protocols, in fact, well explains the increased network density of the DN PDMAPS 1.0;4.0;***5.5h***/PAAm 2.0;0.1, compared to the DN PDMAPS 1.0;4.0;***1h***/PAAm 2.0;0.1, which can be deduced from the decreased swelling equilibrium ratios (Table 1, line IV). Logically, the microhardness values decrease in the same order.

DN hydrogel characterization

Using the Hertz contact theory, the elastic moduli of the DN hydrogels were determined (Table 2). These are also a measure of the hydrogel hardness. From the elastic modulus, one can determine the network density C_x using equation (6). All these parameters obtained for the DNs and for the two SNs are presented in Table 2.

(1) As expected, the increase of the HDSN cross-linking density results in a higher elastic modulus. This result finds a clear explanation in the cross-linking density values, since the DN PDMAPS 1.0;***5.0***/PAAm 2.0;0.1 has a higher junction point density than the DN PDMAPS 1.0;***3.0***/PAAm 2.0;0.1 (Table 2, line I). Here also, a good agreement is observed between the two methods that have been used for the network density evaluation, namely the equilibrium swelling ratio (Table 1) and the junction point density, as determined from the elastic modulus (Table 2).

It should be mentioned that the neat LDSN has the lowest elastic modulus and is, therefore, the softest hydrogel, in contrast to the neat HDSN, which has the highest elastic modulus and the highest hardness (although this could not be measured due to the cracking phenomena mentioned above).

The "softening" effect observed for DN PDMAPS 1.0;***5.0***/PAAm 2.0;0.1, as compared to the neat HDSN, is due to the elasticity imparted into the DN properties by the LDSN. As expected, the hydrogel elastic modulus values are in agreement with the network densities (Table 2, line I).

The morphology of the DN appears to be strongly influenced by the density of the HDSN when it is the first formed SN. In Figures 2A and 2B this influence is clearly demonstrated. The SEM micrograph in Figure 2A represents the surface of the dried DN PDMAPS 1.0;**3.0**/PAAm 2.0;0.1.

Tab. 2. Elastic modulus and network densities for DN hydrogels in the equilibrium swelling state, obtained according to the Hertz contact theory.

Sample	Elastic modulus in MPa	Network density x10^7 in mol/cm^3
I. Influence of the cross-linking agent concentration used to form HDSN		
PDMAPS 1.0;***5.0***/PAAm 2.0;0.1	5.23±0.10	3.5
PDMAPS 1.0;***3.0***/PAAm 2.0;0.1	3.07±0.03	2.1
PAAm 2.0;0.1 (LDSN)	1.575±0.007	1.1
PDMAPS 1.0;4.0 (HDSN)	11.2±0.4	7.7
II. Influence of the monomer concentration ratio in the two SNs and of the LDSN cross-linking density		
PDMAPS 1.0;5.0/PAAm ***2.0***;0.1	5.23±0.10	3.5
PDMAPS 1.0;5.0/PAAm ***3.0***;0.1	2.63±0.04	1.8
III. Influence of the reverse order of DN formation		
PDMAPS 1.0;4.0/PAAm 2.0;0.1 **(“straight” DN)**	15.76	11
PAAm 2.0;0.1/PDMAPS 1.0;4.0 **(“reverse” DN)**	2.80±0.01	1.9
IV. Influence of the time for HDSN cross-linking		
PDMAPS 1.0;4.0- ***1h***/PAAm 2.0;0.1**	6.02±0.05	4.0
PDMAPS 1.0;4.0 – ***5.5h***/PAAm 2.0;0.1**	15.76	11

* The varied parameters for the different DNs are marked with **bold** and *italic*

** Time of for the HDSN cross-linking

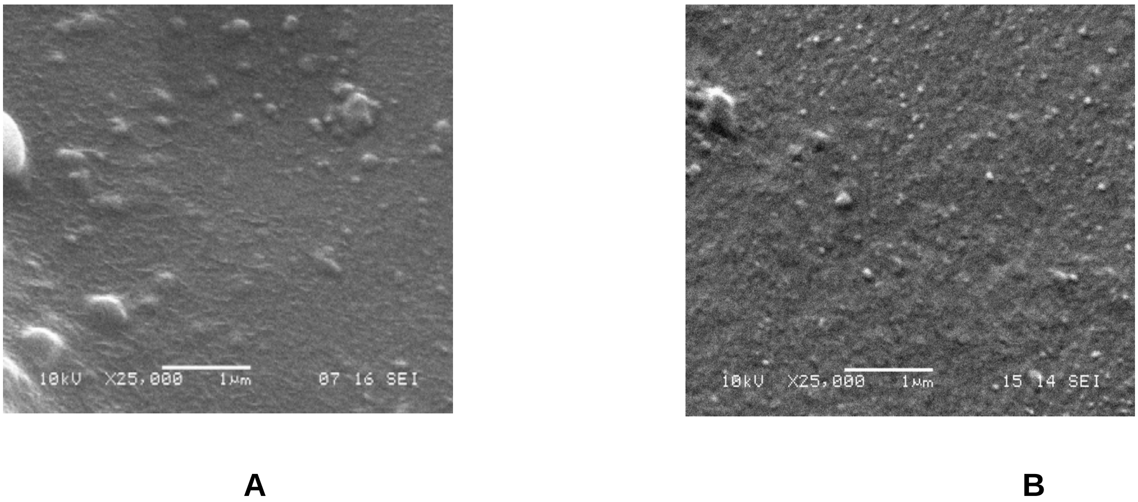

A

B

Fig. 2. SEM micrographs of DN PDMAPS 1.0;3.0/PAAm 2.0;0.1 **(A)** and DN PDMAPS 1.0;5.0/PAAm 2.0;0.1 (**B)** Magnification 25 000 X.

For this DN, the HDSN is produced at a lower concentration (3 mol %) of the cross-linking agent. Therefore, the microphase separation [10] during the formation of the second SN (PAAm LDSN) in this case proceeds easier than that when the concentration of this agent is higher (5 mol %).

As a result, the PAAm inclusions are larger in size at 3 mol% of cross-linking agent (Fig. 2A) than those obtained with 5 mol% of the same agent (Fig. 2B). It is supposed that the more uniform size distribution of the PAAm isles in the latter case is a reason for the higher values of the elastic modulus and network density (Table 2), and microhardness (Table 1) as well as for the lower equilibrium swelling ratio (Tab. 1), as compared to those for the dry DN and DN hydrogel produced with 3 mol% cross-linking agent.

(2) The increase in the LDSN junction points density, i.e., decrease in its monomer concentration, results in an increase of the total network density, as seen in Table 2, line II. This change coincides with the network density variation observed for the same samples, as detected by the equilibrium swelling ratio (Table 1, line II). The network density increase explains very well the higher elastic modulus of DN PDMAPS 1.0;5.0/PAAm ***2.0***;0.1, as compared to PDMAPS 1.0;5.0/PAAm ***3.0***;0.

(3) The influence of the order of SN formation on the mechanical performance of DN hydrogels is shown in Table 2, line III. Both DN samples PDMAPS 1.0;4.0/PAAm 2.0;0.1 (“straight” DN) and DN PAAm 2.0;0.1/PDMAPS 1.0;4.0 (“reverse” DN) have the same composition and cross-linking times and differ only in the order of SN formation. However, it is obvious that the order of formation has a strong effect as the elastic modulus decrease more than three times when only it was changed, the other parameters remaining constant. The network density of the **“**straight**”** DN is almost 6 times higher than that of the **“**reverse**”** one (Table 2, line III). The same trend is deduced from the equilibrium swelling ratios (Table 1, line III) where the **“**straight**”** DN shows a 1.5 times lower equilibrium swelling ratio than the **“**reverse**”** one. Most probably, this is due again to the difference between the PAAm isle size distribution in the both (“straight” and “reversed”) DNs mentioned in the previous section (Figure 1).

(4) The cross-linking time for HDSN formation has also a strong effect on the DN mechanical performance, when in dry state (Table 2, line IV). DN PDMAPS 1.0;4.0 – ***5.5h***/PAAm 2.0;0.1 has more than 2 times higher elastic modulus and hardness, which can be related to its more than 2 times denser network.

Experimental part

Materials

For the production of the SN, two different monomers, i.e. N-(3-sulfopropyl)-N-methacroyloxyethyl-N,N-dimethylammonium betaine (DMAPS) and acrylamide (AAm) have been purchased from Merck, Germany. Potassium persulfate $K_2S_2O_8$ (as an initiator) and methylene-bis-acrylamide (MBAA) (as cross-linking agent) were purchased from Fluka, Switzerland.

Synthesis of DN from DMAPS and AAm

The DN synthesis followed the procedure described earlier (Gong et al. [2]). Four parameters of this synthesis (cross-linking agent concentration used for HDSN preparation; density of LDSN cross-linking, the sequence of HDSN and LDSN formation; time for HDSN cross-linking) have been varied (Table 3). Consequently, their influence on the DNs mechanical performance has been also followed.

Tab. 3. Conditions for DN synthesis and their symbols.

DN symbols	Components of the first SN			Components of the second SN		
	[Monomer] in M	[MBAA] in mol %	Time of cross-linking in h	[Monomer] in M	[MBAA] in mol %	Time of cross-linking in h
PDMAPS 1.0;3.0/ PAAm 2.0;0.1***	1**	3	5.5	2*	0.1	8
PDMAPS 1.0;4.0/ PAAm 2.0;0.1 "straight"DN***	1**	4	5.5	2*	0.1	8
PDMAPS 1.0;5.0/ PAAm 2.0;0.1***	1**	5	5.5	2*	0.1	8
PDMAPS 1.0;5.0/ PAAm 3.0;0.1	1**	5	5.5	3*	0.1	8
PAAm 2.0;0.1/ PDMAPS1.0;4.0 "reverse"DN***	2*	0.1	8	1**	4	8
PDMAPS 1.0;4.0/ PAAm 2.0;0.1***	1**	4	1	2*	0.1	7
HDSN PDMAPS1.0;4.0***	1**	4	5.5	-	-	-
LDSN PAAm 2.0;0.1***	2*	0.1	8	-	-	-

* The used monomer is AAm

** The used monomer is DMAPS

*** 0.1 mol % is the concentration of the initiator used for the production of the SNs and the DNs

Influence of the cross-linking agent concentration used for HDSN preparation

Four aqueous solutions, 5 ml each, of 1M DMAPS, containing 5 mol %, 4 mol %, 3 mol % and 2 mol % MBAA as cross-linking agent, respectively, and 0.1 mol % $K_2S_2O_8$ as initiator, were prepared and poured into a polystyrene Petri dish with a diameter of 3.5 cm. The cross-linking polymerization took place at 72^{o}C for 5.5 h. The HDSN prepared in this way**,** was then swelled (without preliminary washing) in an aqueous solution of 2M AAm, 0.1 mol % MBAA and 0.1 mol % $K_2S_2O_8$ for 24 h. Then, the swollen network was taken out of the solution and put in an oven at 72^{o}C for 8 h, so that the LDSN could be formed in the presence of the already existing HDSN. The two cross-linking polymerization procedures were performed in air atmosphere. Finally, the low molecular weight contaminants (residual initiator, monomer and cross-liking agent) were washed out from the obtained DNs with distilled water at room temperature for 12 days. The absence of the monomer and cross-linking agent in the waste waters was confirmed by means of UV measurements.

Influence of the monomer concentration ratio in the two SNs and of the LDSN cross-linking density

As a result of the attractive (dipole-dipole) interaction between the zwitterionic monomer units in PDMAPS HDSN, the AAm (the monomer, forming the second LDSN) diffusion is retarded, as compared to that of the same in the PAMPS HDSN. Therefore, it was interesting to change the AAm concentration for the control of the AAm gradient and the swelling rate of the PDMAPS network with AAm. To this aim two HDSN were prepared in a similar way as described above. The concentrations of the monomer, cross-linking agent and the initiator were as follows: 1M DMAPS, 5 mol % MBAA and 0.1 mol % $K_2S_2O_8$. The polymerization and cross-linking reaction took place at 72^{o}C for 5.5 h. In order to vary the concentration ratio of the monomers of the two SNs and the LDSN density, the concentration of the monomer, used for preparation of the latter, was changed. The two obtained HDSN, have been swelled without preliminary washing in the following two aqueous solutions: 2M AAm, 0.1 mol % MBAA, 0.1 mol % $K_2S_2O_8$, and 3M AAm, 0.1 mol % MBAA, 0.1 mol % $K_2S_2O_8$, respectively. The formation of the LDSN has been carried out at 72^{o}C for 8 h, and the two DNs obtained have been purified in a similar way as described above.

Influence of the order of HDSN and LDSN formation

The “straight” DN was synthesized by the above described procedure. The “reverse” DN formation starts with the preparation of the LDSN. Using an aqueous solution of 2M AAm, 0.1 mol % MBAA and 0.1 mol % $K_2S_2O_8$, LDSN was synthesized at 72^{o}C for 8 h. Then, it was swelled without preliminary washing for 24 h in an aqueous solution of 1M DMAPS, 4 mol % MBAA, 0.1 mol % $K_2S_2O_8$, and the HDSN was obtained in the presence of the LDSN at 72^{o}C for 5.5 h. The two cross-linking polymerization procedures were performed in air atmosphere. Low molecular contaminants were washed out from the produced “reverse” DN with distilled water for 12 days.

The compositions of the two (“straight” and “inverse”) DNs follow the monomer concentration ratios. They were determined gravimetrically by the yield after each cross-linking polymerization during the preparation of the two DNs. To this purpose, the produced SNs and DNs are dried under vacuum at room temperature.

Influence of the time for HDSN cross-linking

In order to ensure more homogeneous mixing between the two SNs, we have varied the cross-linking time for the first SN formation (in the case of the "straight" DN this is HDSN). Two aqueous solutions, 5 ml each, have been prepared with concentrations of 1M DMAPS, 4 mol % MBAA and 0.1 mol % $K_2S_2O_8$. They have been cross-linked in the presence of air at 72^0C for 1 h and 5.5 h, respectively. For the shorter cross-linking time, the full conversion of the first monomer was not reached; the components for the formation of the second SN (2M AAm, 0.1 mol % MBAA and 0.1 mol % $K_2S_2O_8$) were added to the mixture composed of the aqueous solution of the partly cross-linked first polymer, the linear oligomers and the residual first monomer. The latter can also take part in the formation of the second SN. Polymerization and cross-linking of the LDSN was performed as usual at 72°C for 8 h in air atmosphere. Low molecular contaminants were washed out from the obtained DNs with distilled water for 12 days at room temperature.

Methods for DN characterization

-Microhardness

The microhardness of the dry DNs as well as of the neat SNs were tested with an apparatus for Vicker's microhardness measurements (Leica VMHT, Leica Mikrosysteme GmbH, Wien, Austria) at three different loads: 0.15, 0.25 and 0.5 N. At each load, 5 indentations have been made and the results obtained for the diagonals of the indentation marks were averaged. From the slope of the $P = f(d^2)$ dependence, where P is the load in N and d is the diagonal in m, the Vicker's microhardness value (HV) in MPa is determined, using the following equation:

$$HV = 1.854\ (P/d^2) \qquad (1)$$

Here, 1.854 is a constant reflecting the geometry of the pyramidal diamond indenter used for the Vicker's hardness measurements. This value of *HV* is independent of the load used for measuring the HV. However, because of the elasticity of some the samples, elastic recovery (ER) occurs after sample unloading. As a result of the ER effect, the measured imprint diagonals decrease and the calculated HV-values (Eq. (1)) are higher than the real ones. The necessary corrections to these values could be introduced by the extrapolation to zero load of the ER values measured at different loads, and the extrapolated ER value is added to the measured diameter of the indentations marks.

-Equilibrium swelling ratio

Pieces of the DNs with a fixed size and geometry (triangles) were weighed after drying. Then, the pieces were immersed into distilled water (150 ml) for 4 days in order to reach the equilibrium swelling state. After 4 days, the weight of the samples practically did not change further. The equilibrium swelling ratio was determined, by applying the following relationship:

$$SR = (w_{sw}-w_d)100/w_d \qquad (2)$$

Here, w_{sw} and w_d are the weight of the sample in the swollen and in the dry state, respectively.

-Scanning Electron Microscopy (SEM)

The morphology of dry DN films has been studied by SEM (JEOL Scanning Electron Microscope 5510, Japan). The samples were preliminary coated by a thin gold film in an inert atmosphere (Sputter Coater JEOL Fine Coater 1200, Japan).

-Elastic modulus and hardness of DN hydrogels according the Hertz Contact Theory

The elastic modulus and the hardness of the hydrogels in the equilibrium swelling state have been determined using the Hertz contact theory (e.g., Henderson et al., e.g., Tamagawa et al. [5, 6]). This theory makes use of the contact between a hard ball (ceramic or metal) and a soft surface (elastomeric or hydrogel in our case, see Scheme 1). On the contact surface between the ball and the hydrogel a certain stress σ is induced:

$$\sigma = w\, g/S \tag{3}$$

which is usually taken as a measure for the hydrogel hardness (e.g., Henderson et al. [5]). Here, w is the weight of the ball, g is the gravity acceleration, S is the contact surface area between the ball and the hydrogel. The elastic modulus E of the hydrogel is calculated using the relationship

$$E = (9/16)(r\, w\, g)/R^3_{cont}, \tag{4}$$

Where r is the radius of the ball and R_{cont} is the radius of the contact surface between the ball and the hydrogel (see Scheme 1).

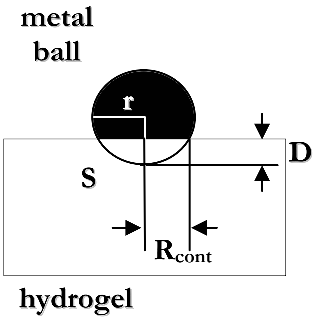

Scheme 1. Hydrogel elastic modulus measurement according to the Hertz contact theory [5].

By measuring the penetration D of the ball into the hydrogel with a cathetometer (Scheme 1), it is possible to calculate R_{cont} , S, σ and E, respectively. The conditions for the validity of the contact theory (all deformations are purely elastic, all elastic moduli remain unchanged; both materials in contact are elastically isotropic and the curvature of the ball at the contact point is a paraboloid (e.g., Schwarz [7])) are fulfilled for the samples studied. From the value of the elastic modulus, the total density of the DNs was calculated

$$E = 6 C_x R T, \tag{5}$$

where E is the elastic modulus in dyne/cm^2; T is the temperature in K; R is the universal gas constant in dyne.cm/mol.K; C_x is the cross-link density in moles cross-links/cm^3.

Acknowledgements

This research was supported through DAAD Project No DAAD-06/2005.

References

[1] Mott, P. H.; Roland, C. M.; *Macromolecules* **2000**, *33*, 4132-4137.
[2] Gong, J. P.; Katsuyama, T.; Osada, Y.; *Adv. Mater.* **2003**, *15*, 1155-1158.
[3] Lowe, A. B.; Vamvakaki, M.; Wassall, M. A.; Wong, L.; Billingham, N. C.; Armes, S. P.; Lloyd, A.W.; *J. Biomed. Mater. Res.* **2000**, *52*, 88–94.
[4] Ishihara, K.; Nomura, H.; Mihara, T.;Kurita, K.; Iwasaki, Y.; Nakabayashi, N.; J. Biomed. Mater. Res. **1998**, *39*, 323–330.
[5] Henderson, G. V. S.; Campbell, D. O.; Kuzmicz, V.; Sperling, L. H.; *J. Chem. Edu.* **1985**, *62 (3)*, 269-270.
[6] Tamagawa, H.; Nogata, F.; Yagasaki, K.; *J. Coll. Interf. Sci.* **2004**, *275*, 107-112.
[7] Schwarz, U. D.; *J. Coll.& Interf. Sci.* **2003**, *261*, 99-106.
[8] Sawyer, L. C.; Grubb, D.T.; *"Polymer Microscopy"*, Chapman and Hall, **1987**, pp. 95.
[9] Georgiev, G. S.: Kamenska, E. B.; Vassileva, E. D.; Kamenova, I. P.; Georgieva, V. T.; Iliev, S. B.; Ivanov, I. A.; Biomacromoilecules, **2006**, *7*, 1329 -1334.
[10] Tsukeshiba, H.; Huang, M., Na, Y.; Kurokawa, T.; Kuwabara, R.; Tanaka, Y.; Furukawa, H.; Osada, Y.; Gong, J.; J. Phys. Chem., **2005**, *B 109*, 16304-16309.